INTERNATIONAL JOURNAL OF AGRICULTURE & BIOLOGY
ISSN Print: 1560–8530; ISSN Online: 1814–9596
20F–142/2021/25–2–327–337
DOI: 10.17957/IJAB/15.1672
http://www.fspublishers.org

Full Length Article

Genome-Wide Identification and Expression Analysis of the *NRAMP* Family in Melon

Lan Jin[1,2], Bayaer Enhe[2], Yufeng Zhuang[2], Agula Hasi[1*] and Feng Gao[2*]
[1]*Key Laboratory of Herbage and Endemic Crop Biotechnology (Inner Mongolia University), Ministry of Education, College of Life Sciences, Inner Mongolia University, Hohhot 010070, China*
[2]*College of Life Science and Technology, Inner Mongolia Normal University, Hohhot 010022, China*
[*]For correspondence: hasind@sina.com; imgaofeng@163.com
Received 15 August 2020; Accepted 15 October 2020; Published 10 January 2021

Abstract

The NRAMPs (natural resistance-associated macrophage proteins) are evolutionarily conserved integral membrane proteins that transport a broad range of metal ions. A comprehensive analysis of NRAMP family genes has not been reported for melon (*Cucumis melo*). In this study, six *CmNRAMP* genes were identified from the melon genome. Analyses of gene structure, phylogeny, chromosome location and conserved motifs revealed two groups of CmNRAMPs: one group contained only CmNRAMP5, which had 12 conserved motifs like NRAMPs in *Arabidopsis thaliana* and rice (*Oryza sativa*). The other group contained five CmNRAMPs and all had shorter amino acid sequences compared with CmNRAMP5. Expression analyses suggested that CmNRAMP genes are expressed differently in response to treatments with different plant hormones, abiotic factors, and metals (iron, copper, and manganese). The most responsive gene was *CmNRAMP5*, which showed significant changes in its transcript levels in response to abscisic acid (ABA), indole acetic acid, cytokinin, methyl jasmonate, brassinosteroid, Fe, and Cu. The least responsive gene was *CmNARMP6*, which was only significantly responsive to ABA, Fe, and Mn. These results indicate that *CmNRAMP* genes function in numerous tissues and at different developmental stages. A protein–protein interaction analysis indicated that CmNRAMPs interact with proteins involved in transmembrane transport, superoxide dismutase activity, plant hormone signal transduction, signal transduction by protein phosphorylation, and nicotianamine synthase activity. This study provides valuable insights into the potential function of *CmNRAMP* genes and their encoded products.

Keywords: *Cucumis melo*; Expression analysis; NRAMP gene family; Protein-protein interaction

Introduction

Natural resistance-associated macrophage proteins (NRAMPs) are a highly evolutionarily conserved family of integral membrane proteins that are widely distributed among diverse organisms, including bacteria, yeast, algae, plants and animals (Nevo and Nelson 2006). The first *NRAMP* gene, *NRAMP1*, was identified in mammals, and was found to be expressed in phagosomes of infected macrophages (Vidal *et al*. 1993). The NRAMPs participate in resistance to bacterial infection by transporting metal ions such as manganese (Mn^{2+}) and iron (Fe^{2+}) (Supek *et al*. 1996; Fleming *et al*. 1997). The wide distribution of NRAMPs among different species indicates the importance of their function. Subsequent studies have shown that NRAMPs exhibit functional divergence and broad substrate specificity in different species. Various members of the NRAMP family function as proton-coupled metal ion transporters to transport manganese (Mn^{2+}), iron (Fe^{2+}), zinc (Zn^{2+}), copper (Cu^{2+}), cadmium (Cd^{2+}), nickel (Ni^{2+}), cobalt (Co^{2+}), and aluminum (Al^{3+}) (Colangelo and Guerinot 2006; Nevo and Nelson 2006; Xia *et al.* 2010; Sasaki *et al.* 2012; Xiong *et al.* 2012; Li *et al.* 2014). These proteins have been implicated in the uptake, translocation, intracellular transport, and detoxification of transition metals (Nevo and Nelson 2006). The transport of metal ions in plants plays important roles in plant growth, development, signal transduction, nutrition, and protection against heavy metal poisoning. However, most studies on NRAMPs have been conducted in yeast, and their exact physiological roles in plants are still poorly understood.

Melon (*Cucumis melo* L.) is an economically important and widely cultivated vegetable crop (Huang *et al*. 2016; Xiong *et al*. 2018) and is an ideal model for analyzing the development and ripening of fleshy fruits (Pech *et al.* 2008; Ezura and Owino 2008). However, great economic losses are caused by biological and abiotic stresses such as diseases and adverse environmental conditions. In our previous study using suppression subtractive hybridization (SSH) analyses, we found that an expressed sequence tag

(EST) (MELO3C019215) encoding a NRAMP was differentially expressed during the ethylene climacteric burst in melon fruit (Gao *et al*. 2013).

In this work, the *CmNRAMP5* gene fragment was used to identify all *NRAMP*-like gene sequences in the melon genome. Then, the expression patterns of *CmNRAMP* genes in different tissues at different stages, and in response to different hormones, stress, and metal ions were determined. Finally, to further understand the potential functions of these proteins, a protein–protein interaction network was constructed.

Materials and Methods

Identification of NRAMP family genes in melon

All candidate *CmNRAMP* genes were derived from the melon genome database (Zheng *et al*. 2019) using BLASTp searches. The search query was the *NRAMP* EST isolated from SSH libraries in our previous study (Gao *et al*. 2013). The predicted amino acid sequences of the candidate proteins were searched to identify NRAMP domains using the Simple Modular Architecture Research Tool (SMART) (Letunic and Bork 2018). Only the sequences with a full-length NRAMP domain were considered as CmNRAMPs and used for further analyses.

Sequence alignment, phylogenetic analysis and conserved motif analysis

Multiple sequence alignment of the identified CmNRAMP sequences was performed using Clustal W with default parameters and was adjusted manually. Phylogenetic trees were drawn with MEGA 5.10 software using the neighbor-joining method, and the reliability of the obtained trees was assessed with a bootstrap value of 1000 (Tamura *et al*. 2011). Conserved motifs were identified using MEME v. 5.1.1 (http://meme-suite.org/tools/meme) with the following parameters: maximum number of motifs: 12, motif width >6 and <200 (Bailey *et al*. 2009). The functional interaction networks of proteins were constructed using tools at the STRING protein interaction database (http://string-db.org/) with the confidence parameter set at 0.15 and threshold set at 75. The resulting interaction information was directly imported into Cytoscape software (3.7.2) for visual editing (Shannon *et al*. 2003; Szklarczyk *et al*. 2019).

Promoter analysis and determination of chromosomal locations

The *cis*-acting regulatory elements in the promoter of the *NRAMP* gene were identified using tools at the PlantCARE database (Lescot *et al*. 2002). The promoter region was defined as the 2-kb sequence upstream of the transcription start site. Using the sequences of the melon genome and *NRAMP* genes, we used TBtools software (Chen *et al*. 2018) to map the *NRAMP* genes onto the chromosomes.

Plant materials and treatments

Melon (*C. melo* L. cultivar Hetao) plants were grown in the field and the mesocarp of fruit (0 to 50 days after pollination; DAP) and internal ethylene were collected as described previously (Gao *et al*. 2013). Other tissues, such as roots, stems, young leaves, and flowers were also collected from greenhouse-grown plants. To minimize the effects of endogenous hormones on *CmNRAMP* transcription, sterile young leaves were transferred to 250-mL flasks containing 100 mL of ½-strength Murashige and Skoog (MS) liquid medium containing the treatment substance. All plant materials were sampled in three replicates. The flasks were incubated on a rotary shaker with shaking (100 rpm) for 2 h at 30°C. The treatments were indole acetic acid (IAA, 0, 0.4, 4, 40 μM), gibberellic acid (GA_3, 0, 0.4, 4, 40 μM), salicylic acid (SA, 0, 100, 500, 1000 μM) cytokinin (CTK, 6-benzylaminopurine, 6-BAP, 0, 0.4, 4, 40 μM), abscisic acid (ABA, 0, 0.4, 4, 40 μM), brassinosteroid (BR, 0, 0.01, 0.05, 0.1 mg/L), peroxide (H_2O_2, 0, 1×10^4, 2×10^4, 4×10^4 μM), methyl jasmonate (MeJA, 0, 4.46, 44.6, 446 μM) and metal ions of Fe^{2+} (0, 50, 100, 200 mg/L), Cu^{2+} (0, 50, 100, 200 mg/L), and Mn^{2+} (0, 0.272, 1.36, 6.8 mg/L) at different concentrations. Leaves were cultured in basal medium without any additive as the control. At the end of the culture, all leaves were removed, blotted dried, frozen in liquid nitrogen and then stored at −80°C until RNA analysis.

RNA isolation and qRT-PCR analysis

Total RNA was extracted from plant samples using RNAiso for polysaccharide-rich plant tissue (Takara, Otsu, Japan) as per manufacturer's instructions. All RNA extracts were analyzed by agarose gel electrophoresis and UV spectrophotometry.

The *CmNRAMP* mRNA levels were measured by quantitative PCR (qPCR). The primers (Table 1) were designed using Primer Premier v. 5.0, avoiding the conserved regions of the NRAMP motif and focusing on intron regions to reduce potential DNA contamination. For each trial, nine independent experiments were conducted (each experiment had three biological replicates, and each sample was analyzed with three technical replicates). All relative -fold differences in expression were normalized to the transcript level of *GAPDH*.

First-strand cDNA was synthesized using the PrimeScript® RT reagent kit with gDNA eraser (Perfect Real Time; Takara) following the manufacturer's protocol. For cDNA synthesis, 0.5 μg of total RNA from each sample was used as template in a 10-μL reaction mixture. SYBR® Premix Ex Taq™ II (Tli RNaseH Plus; Takara) was used for real-time RT-PCR, with 5 μM of each primer, and the reactions were run on a Mastercycler® ep realplex (Eppendorf, Hamburg, Germany). Melting curves were generated immediately after the last cycle to exclude any influence of primer dimers. Cycle numbers at which the

Table 1: Sequences of primers used in qRT-PCR

Gene name	Gene ID	Forward primer sequence (5'-3')	Reverse primer sequence (5'-3')	Product size (bp)
CmNramp5	MELO3C019215	CTTGACGGAGAAGGTTGTGGTAAT	TGGCCGAAAGCAACTGGATC	248
CmNramp6	MELO3C026742	GAGAAATGAAGGGAGGGAGGTT	GAAGAAGGTGGATTCGACAAGC	99
CmNramp1	MELO3C023938	GTAAAGCTGAGTACCCCAAGGC	CACCAAACAGGAATGCGGAAG	136
CmNramp2	MELO3C000512	ATCATTGGTGGGTCTTCTGGG	CCATCTTGGCCTTACTGCTTG	121
CmGAPDH	AB033600	ATCATTCCTAGCAGCACTGG	TTGGCATCAAATATGCTTGACCTG	278

Table 2: The information including amino acid length, number of exons and introns, and chromosomal assignment of six *CmNRAMP* and *CmEIN2* genes

Gene	Gene identification	Location	Chromosome (no.)	Protein length (no. of amino acids)	Exons (no.)	Introns (no.)
CmNRAMP1	MELO3C023938	24502353-24505332	4	324	9	8
CmNRAMP2	MELO3C000512	15521339- 15522187	0	73	2	1
CmNRAMP3	MELO3C010638	7913869-7915404	3	310	7	6
CmNRAMP4	MELO3C021848	6615332-6617251	11	283	5	4
CmNRAMP5	MELO3C019215	9194803-9198277	11	510	4	3
CmNRAMP6	MELO3C026742	25044787- 25048409	4	324	10	9
CmEIN2	MELO3C014230	29460142- 29457492	8	1291	7	6

fluorescence passed the cycle threshold (Ct) were analyzed, and relative expression was calculated by the $2^{-\Delta\Delta Ct}$ method. The differences were analyzed using DPS (Data Processing System) software (Tang and Zhang 2013).

Results

Gene identification and sequence analysis

We mapped the chromosomal locations of the genes based on the location information shown in Table 2, using TBtools software (Fig. 1). *CmNRAMP1* and *CmNRAMP6* were located on chromosome 4, *CmNRAMP4* and *CmNRAMP5* were located on chromosome 11 and the rest were located on different chromosomes.

Next, we analyzed the phylogenetic relationships between melon *NRAMP* genes and their homologs in *A. thaliana* and *O. sativa*. The tree had two large groups, in which both monocots and dicots were distributed (Fig. 2, Table S1). One group contained *OsNRAMP1/6/5/4/3*, *AtNRAMP1/6*, *CmNRAMP3/4*, and *CmNRAMP1/6*. OsNRAMP6/5/4/3 and AtNRAMP1/6 are plasma membrane-localized proteins. In rice, OsNRAMP4 (NRAT1) functions as a transporter specific for trivalent Al^{3+} (Xia *et al*. 2010; Li *et al*. 2014); OsNRAMP5 plays a role in the uptake of Mn^{2+}, Fe^{2+}, and Cd^{2+} from the soil (Sasaki *et al*. 2012); OsNRAMP6 is involved in uptake of Fe^{2+} and Mn^{2+}, and contributes to disease resistance (Peris-Peris *et al*. 2017); and OsNRAMP3 functions as a switch in response to environmental Mn^{2+} changes (Yamaji *et al*. 2013). In *Arabidopsis*, AtNRAMP1/6 mediates Mn^{2+} uptake and Cd^{2+} toxicity, respectively (Cailliatte *et al*. 2009, 2010). The other group contained *CmNRAMP5*, *AtNRAMP2/3/4/5* and *OsNRAMP2/7*. AtNRAMP3/4 are functionally redundant, and transport Fe^{2+} and Mn^{2+} and the toxic metal ion Cd^{2+} (Lanquar *et al*. 2005). AtNRAMP2 transports Mn^{2+} via the trans-Golgi network to support reactions in photosynthesis and cellular redox homeostasis (Alejandro *et al*. 2017; Gao *et al*. 2018).

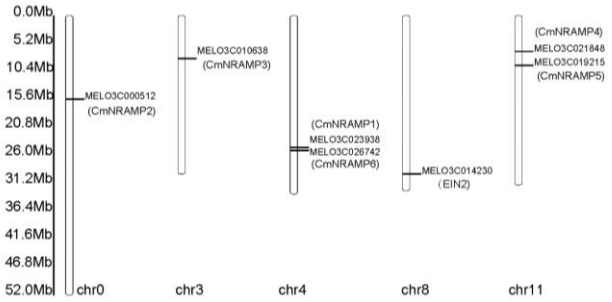

Fig. 1: Chromosomal locations of melon NRAMP genes
Chr represents the chromosomes. The lengths of chromosomes of each NRAMP gene are displayed proportionately. Black lines on bars indicate the locations of NRAMP genes

To further examine the sequence features of plant NRAMPs, we conducted a comparative analysis of the conserved motifs among NRAMPs in melon, *Arabidopsis*, and rice. Twelve motifs were detected in NRAMP amino acid sequences, as revealed by analyses using the MEME program (Fig. S1). In general, NRAMPs that clustered in the same subgroups shared similar motif compositions (Fig. 2), indicating functional similarities among members of the same subgroup. Nearly all of the NRAMP members contained motifs 3, 1, 5, 9, 4, and 6, suggesting that these motifs are important for the functions of NRAMPs. Motif 12 was only present in members of subgroup II. All the members of this group except for AtNRAMP5 contained 12 motifs. Four NRAMPs in melon were shorter than their homologs in other plants. *CmNRAMP3* and *CmNRAMP4* were located on different chromosomes, and their encoded proteins lacked N and C-terminal motifs and the N-terminal motif, respectively. The proteins encoded by *CmNRAMP6* and *CmNRAMP1* contained N-terminal motifs, but only *CmNRAMP5* contained all motifs. The differences in motif distribution among NRAMPs suggested that the functions of their encoded proteins have diverged during evolution.

To better understand the potential regulation of *CmNRAMP* genes, we searched their promoter regions for

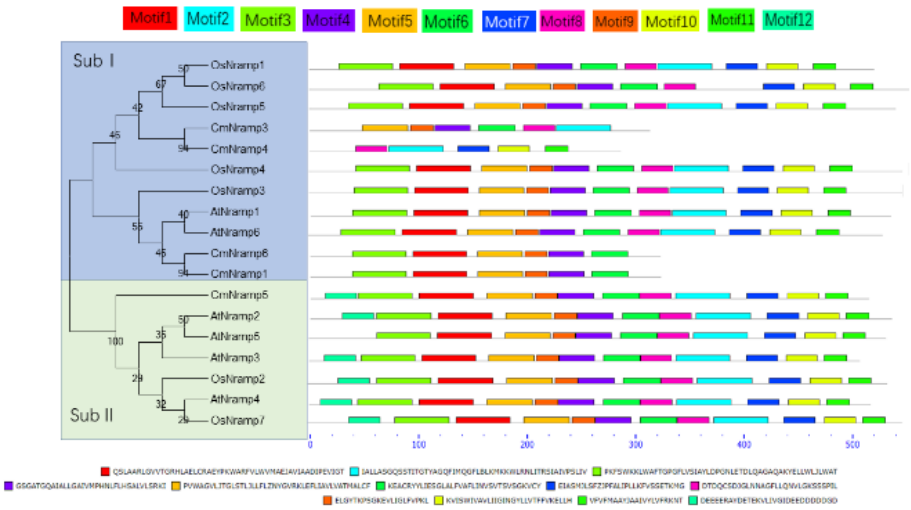

Fig. 2: Motif analysis of NRAMP proteins in *C. melo*, *A. thaliana* and *O. sativa*
A phylogenetic tree was constructed by MEGA5.10. Different subfamilies are marked with different color backgrounds. Motifs in the NRAMP proteins were elucidated by MEME. Different motifs are represented by different colored numbered boxes

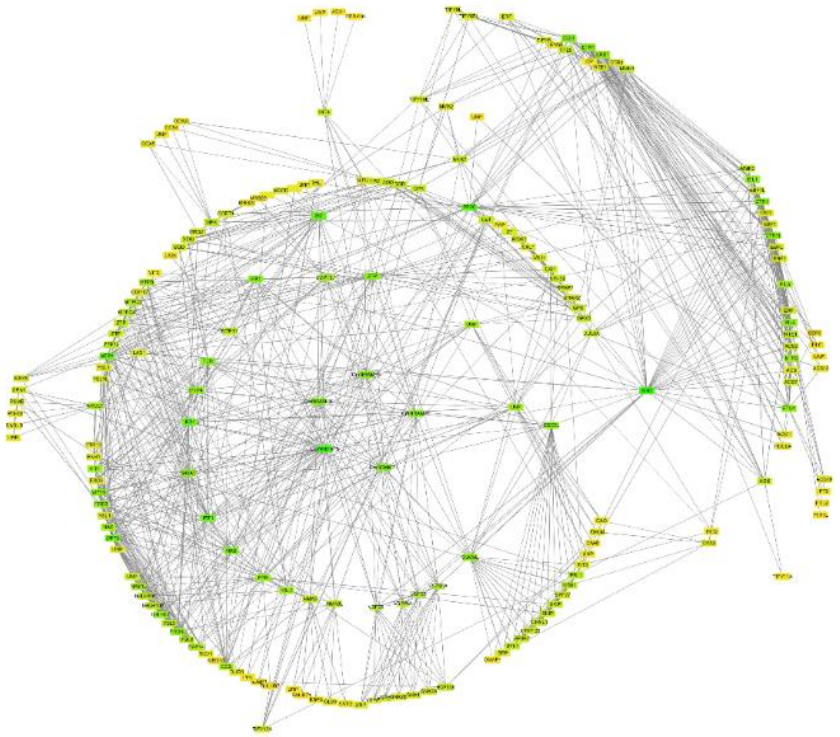

Fig. 3: Functional interaction networks of CmNRAMP proteins in melon according to STRING database and Cytoscape software 3.7.2 (IDARE)

cis-acting elements (Table S2). The promoter regions contained hormone response elements including methyl jasmonate (MeJA)-, gibberellin-, auxin- and SA-response elements; as well as low temperature-, drought-, and light-response elements. The results provided the basis for selecting different exogenous hormones to treat melon for analyses of *CmNRAMP* gene expression patterns.

Protein–protein interaction analysis

To explore the interactions between NRAMPs and other proteins in melon, an interaction network was built. The CmNRAMP sequences were used as queries to obtain interacting protein information in the STRING database and the corresponding value was derived. The protein ID in the

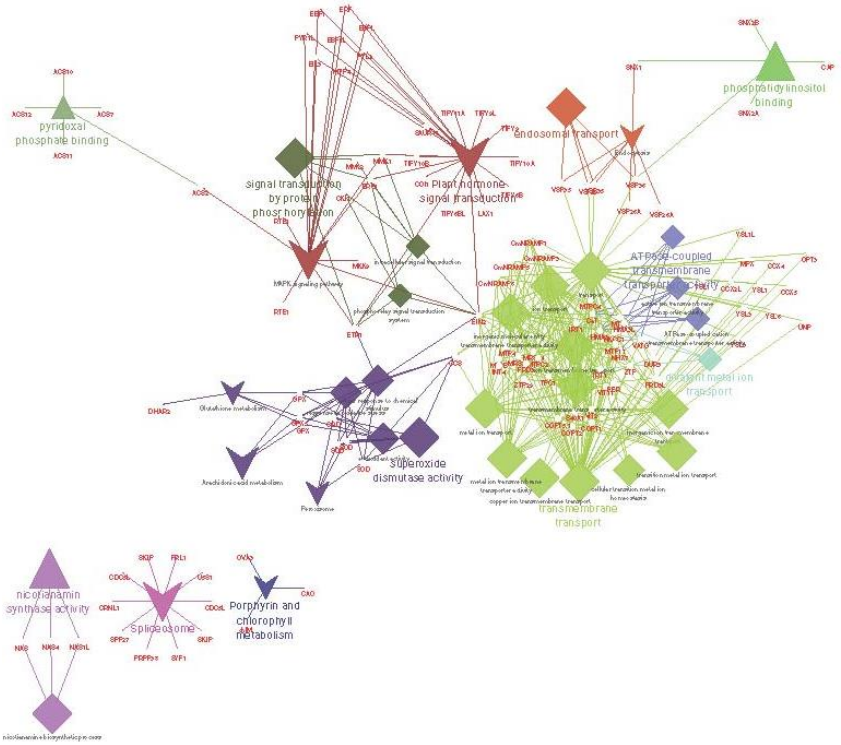

Fig. 4: Functional interaction networks of CmNRAMP proteins in melon according to STRING database and Cytoscape software 3.7.2 (ClueGO)

The parallelogram indicates biological process, triangle indicates molecular function, and V-type indicates KEGG

STRING database was converted into the ID in the Uniprot database, and the network was visualized using Cytoscape.

A total of 192 proteins were obtained from the STRING database to construct the PPI, including proteins that participate in transmembrane transport, superoxide dismutase (SOD) activity, ATPase-coupled transmembrane transporter activity, signal transduction by protein phosphorylation, plant hormone signal transduction, nicotianamine synthase activity, endosomal transport, spliceosomes, porphyrin and chlorophyll metabolism, divalent metal ion transport, phosphatidylinositol binding, and pyridoxal phosphate binding (Fig. 3, Fig. 4, Fig. S2 and Table S3).

The NRAMPs are metal ion transporters, and the dynamic equilibrium of metal ions is known to affect diverse physiological responses. Our network analysis suggested that NRAMPs may play several roles in plant ethylene signal transduction. First, NRAMPs directly interact with VSP and CDC, which interact with EIN2. Second, NRAMPs have indirect interactions, with PP2C and other ethylene signal transduction proteins *via* their interaction with COP5.1 (all CmNRAMPs except CmNRAMP5) or CaT (all NRAMPs), or with EIN2 via their interactions with CaT (all CmNRAMPs).

The protein–protein interaction analysis also indicated that NRAMPs interact with the transcription factors FER and MT to affect SOD activity; and interact with IRT to affect the regulation of some transcription factors (bHLH47, bHLH 92, bHLH 100, bHLH 101). Interactions with HMA3 and HMA3L affect the regulation of GLP (involved in pathogen resistance), SAUR71 (involved in IAA signaling), and CCS (a copper chaperone for SOD). The interaction with CDC5L regulates spliceosomes *via* SYF1, SKIP, U5S1, and PRL1. Only CmNRAMP5 from the NRAMP family may directly interact with NKCC1 for regulation of SPA1, PSMB, PDH51, and DAGLB.

Expression analyses

Only four members of the gene family were annotated in the fruit transcriptome data (unpublished data). The qRT-PCR analyses confirmed that the other two family members were expressed at low levels or not expressed in the leaves. Therefore, the expression patterns of only four *CmNRAMP* genes were analyzed in this study.

Expression profiles of *CmNRAMP* genes in different tissues: The expression patterns of *CmNRAMP* genes in different tissues (roots, stem, leaves, and flowers) or fruit at different developmental stages (every 5 days from 0 to 50 DAP) were analyzed by qRT-PCR to explore their potential functions during the vegetative and reproductive development of melon.

The four analyzed *CmNRAMP* genes were detected in all tissues and showed variable transcript levels (Fig.

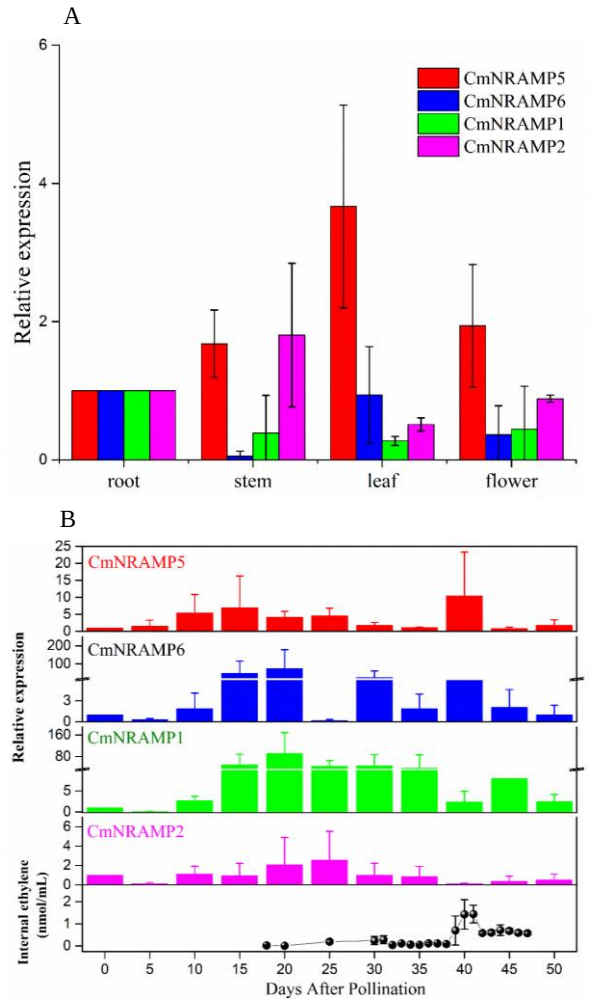

Fig. 5: Expression analysis of selected melon *NRAMP* genes in (**A**) different tissues and (**B**) fruit development stages using quantitative reverse-transcription polymerase chain reaction

5A). The transcript levels of *CmNRAMP 2, 5,* and *6* were the highest in the stem, leaves, and roots, respectively, and their transcript levels in these three tissues were not significantly different. *CmNRAMP1* was abundantly expressed in the roots, and at significantly different levels among other tissues.

CmNRAMP genes showed high transcript levels during the fruit development stage (15–25 DAP), while the transcript level of *CmNRAMP*5 peaked at the same time as the climacteric peak of ethylene production (Fig. 5B). This result indicated that the expression of *CmNRAMPs* is at least partially ethylene-dependent or might be upstream regulator of ethylene.

Expression of *CmNRAMP* genes under different hormone treatments: We determined the changes in the transcript levels of *CmNRAMP* genes in response to treatments with ABA, CTK (6-BAP), BR, IAA, SA, MeJA, and GA at a range of concentrations. The transcript levels were quantified by qRT-PCR (Fig. 6).

Compared with the control group (0 μmol/L), the groups treated with ABA showed significantly decreased transcript levels of *CmNRAMP1, 5,* and *6*. The transcript level of *CmNRAMP2* increased and then decreased with increasing ABA concentrations.

Compared with the control, the groups treated with CTK tended to show decreased transcript levels of *CmNRAMP1, 5,* and *6* while that of *CmNRAMP2* decreased, increased, and then decreased with increasing CTK concentrations. The results indicated that the gene transcript levels were significantly different between the control and the 40 μmol/L CTK treatment, but not among the 0.4 μmol/L, 4 μmol/L and 40 μmol/L treatments. There was no significant difference in transcript levels among *CmNRAMP1, 2* and *6* in each CTK treatment.

In the BR treatment, the transcript level of *CmNRAMP1* increased then decreased, those of *CmNRAMP2* and *6* increased, and that of *CmNRAMP5* decreased, compared with their respective levels in the control. The results indicated that there was no significant difference in transcript levels among *CmNRAMP1, 2,* and *6* at each BR concentration. The transcript level of *CmNRAMP5* showed the largest decrease in the 0.05 mg/L BR treatment, to 0.1 times that in the control group. The results indicated that the transcript level of *CmNRAMP5* differed significantly between the control and the 0.1 mg/L BR treatment, and between the control and the 4 mol/L BR treatment (extremely significant difference), but did not differ significantly among the 0.01 mg/L, 0.05 mg/L and 0.1 mg/L BR treatments.

In the IAA treatment, the transcript levels of the four genes decreased then increased with increasing IAA concentrations. The results indicated that there was no significant difference in transcript levels among *CmNRAMP1, 2,* and 6. The transcript level of *CmNRAMP5* in the 0.4 μmol/L IAA treatment was only 0.31 times that in the control group, but was 12.41 times that in the control group in the 40 μmol/L IAA treatment. The results indicated that the expression level of *CmNRAMP5* differed significantly between the 40 μmol/L and 4 μmol/L IAA treatments, and between the control and the 40 μmol/L IAA treatment (extremely significant difference). There was no significant difference in the *CmNRAMP5* transcript levels among the control and the 0.4 μmol/L and 4 μmol/L IAA treatments.

Treatment with SA increased the transcript levels of *CmNRAMP1, 2, 5,* and 6, compared with the control. The results indicated that the transcript levels of *CmNRAMP6* in the 100 μmol/L and 500 μmol/L SA treatments were significantly different from that in the control. The transcript levels of *CmNRAMP6* did not differ significantly among the other SA treatments.

In the MeJA treatments, the transcript levels of the four genes increased, decreased and then increased. *CmNRAMP2* and 5 had the highest transcript levels in the 4.46 μmol/L treatment, which were 10.64 and 21.61 times that in the

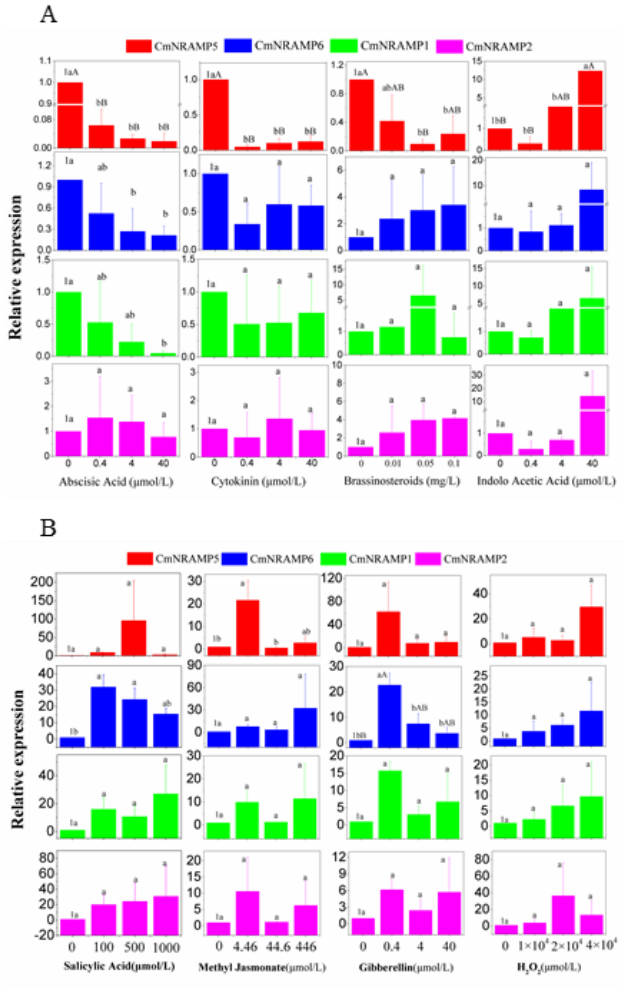

Fig. 6: Expression analysis of selected melon *NRAMP* genes in different hormones and stress treatment using quantitative reverse-transcription polymerase chain reaction (**A** and **B**)

control, respectively. The transcript level of *CmNRAMP5* in the 4.46 μmol/L MeJA treatment was significantly different from those in the control and 44.6 μmol/L MeJA.

In the GA treatments, the transcript levels of the four genes were highest in the 0.4 μmol/L GA treatment. The *CmNRAMP6* transcript levels were significantly different between the 0.4 μmol/L and 4 μmol/L GA treatments, and extremely significantly different between the 0.4 μmol/L GA treatment and the control.

Expression of *CmNRAMP* genes in response to H_2O_2: Treatment with H_2O_2 increased the transcript levels of all *CmNRAMP* genes, compared with the control. There was no significant difference in transcript levels among the four genes (Fig. 6).

Expression of *CmNRAMP* genes under different metal treatments: We determined changes in the transcript levels of *CmNRAMP* genes in melon roots in response to treatments with Mn^{2+}, Cu^{2+}, and Fe^{2+} using qRT-PCR analyses (Fig. 7).

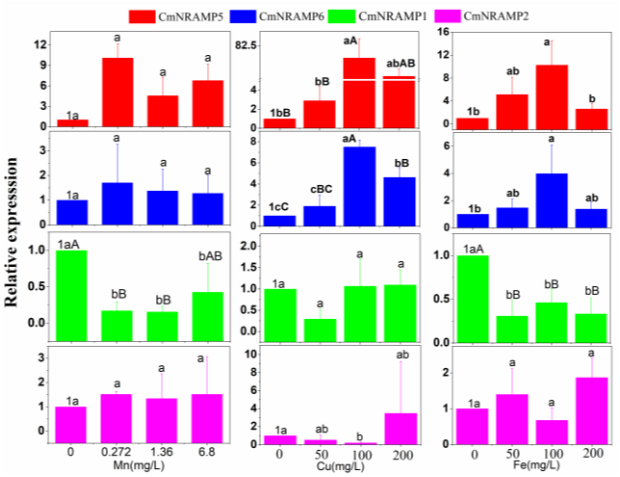

Fig. 7: Expression analysis of selected melon *NRAMP* genes in three heavy metal treatment using quantitative reverse-transcription polymerase chain reaction

Treatments with Mn^{2+} increased the transcript levels of *CmNRAMP5* and *6*, with both showing peak levels in the 0.272 mg/L Mn^{2+} treatment. There was no significant difference in the transcript levels of *CmNRAMP2*, *5*, and *6* among the Mn^{2+} treatments. *CmNRAMP1* was down-regulated by Mn^{2+} treatments, with the lowest transcript level in the 0.272 mg/L Mn^{2+} treatment. The transcript levels of *CmNRAMP1* differed significantly between the control and the Mn^{2+} treatments.

Treatment with Cu^{2+} up-regulated *CmNRAMP5* and *6*, suggesting their encoded proteins have transporter activity in melon. Both genes were most strongly induced in the 100 mg/L Cu^{2+} treatment, and were significantly higher in that group than in the control and other Cu^{2+} treatments. *CmNRAMP2* was down-regulated by Cu^{2+}, with the lowest transcript level in the 100 mg/L Cu^{2+} treatment, where it was significantly lower than that in the control. However, the transcript levels of *CmNRAMP1* were similar among all the Cu^{2+} treatments.

Treatment with Fe^{2+} up-regulated *CmNRAMP5* and *6*, down-regulated *CmNRAMP1*, and did not affected *CmNRAMP2*. These results suggested that *CmNRAMP5* and *6* may have transporter activity in melon. The up-regulated genes were most highly induced by Fe^{2+} at 100 mg/L, and their transcript levels were significantly higher than those in the control. The down-regulation of *CmNRAMP1* was approximately the same among all the Fe^{2+} treatments, and its transcript levels were significantly lower than those in the control.

Discussion

Fruit ripening is regulated by a great deal of stimuli, including light, water availability, plant nutrient status, temperature, and hormones (Gao *et al*. 2013; Huang *et al*.

2016). Melon is an economically important and widely cultivated vegetable crop that provides nutrients in the daily diet of consumers (Bie *et al*. 2017). In plant cells, metal ions are involved in physiological and biochemical reactions, and these reactions are affected by the enrichment and transport of metal ions. Therefore, it is important to study the relationship between metal transporters and the amount of heavy metal residues that accumulate during fruit development. Previous studies have shown that members of the NRAMP carrier family participate in the maintenance of metal homeostasis in *Arabidopsis*, rice, soybean, *Malus baccata*, *Malus xiaojinensis*, peanut, and *Brassica napus* (Xiao *et al*. 2008; Xiong *et al*. 2012; Zha *et al*. 2014; Pan *et al*. 2015; Meng *et al*. 2017; Qin *et al*. 2017). However, no detailed information was available for this family of transporters in melon. Here, we used a bioinformatics approach to identify the members of NRAMP family in the *C. melo* genome and to determine their biological roles during melon development.

In this study, searches of the melon genome revealed six putative *CmNRAMP* genes. Phylogenetic analysis clustered all of their encoded proteins into two distinct subfamilies. The subcellular localization of proteins in the same subfamily was similar among *Arabidopsis*, rice, common bean, and soybean (Qin *et al*. 2017; Mani and Sankaranarayanan 2018; Ishida *et al*. 2018). Interestingly, all of the melon *NRAMPs* except *CmNRAMP5* contained fewer motifs and had shorter amino acid sequences than their homologs in other plants. Only *CmNRAMP5*, which was in its own subfamily, had the 12 characteristic NRAMP motifs.

We detected *cis*-acting elements in the promoter regions of *CmNRAMPs* and monitored changes in gene transcript levels in response to various treatments. These analyses revealed several hormone-responsive elements in the *CmNRAMPs* promoters. In the expression analyses, all the *CmNRAMPs* were up-regulated by SA, especially *CmNRAMP6*. *CmNRAMP1/5/6* were down-regulated by ABA, and all the *CmNRAMPs* were up-regulated by H_2O_2. Treatment with IAA affected the transcript levels of *CmNRAMP5*, while treatment with GA affected the transcript levels of *CmNRAMP6*. *CmNRAMP5* transcript levels were affected by treatments with CTK, MeJA, and BR.

There were significant changes in the transcript levels of *CmNRAMP1/5/6* in response to Fe^{2+}; of *CmNRAMP2/5/6* in response to Cu^{2+}; and of *CmNRAMP1* in response to Mn^{2+}. The closest homologs of *CmNRAMP5* in *Arabidopsis* are *AtNramp3/4*. The transcript levels of *AtNRAMP4* were shown to be greatly increased by 24 and 72 h of exposure to excess Cu (Zlobin *et al*. 2015). Our results and those of other studies indicate that the *CmNRAMPs* play important roles in responses to plant hormones and in maintaining metal ion homeostasis in melon.

NRAMPs are known to transport divalent metal ions, and some of them show functional redundancy, such as AtNRAMP3 and AtNRAMP4 (Lanquar *et al*. 2005). However, some members of the NRAMP family can transport other ions, such as trivalent Al^{3+} (Li *et al*. 2014). Pleiotropy of the NRAMPs can be demonstrated through PPI network analyses, and is fundamental for understanding their function. The ClueGO results indicated that the largest category of proteins in the protein–protein interaction network was transmembrane transporters. Other highly represented proteins were related to SOD activity, signal transduction by protein phosphorylation (MKKs), plant hormone signal transduction (ethylene, auxin, ABA), and spliceosomes (CDC5L) (Fig. 4).

The protein–protein interaction network included proteins involved in plant hormone signal transduction. Several metal ions, especially Cu^{2+} have a critical role in ethylene perception and ethylene signaling (Hirayama and Alonso 2000). Ethylene perception requires Cu^{2+} for binding to ethylene receptors. In addition, EIN2, which has an NRAMP-like motif in N-terminal, plays positive role in ethylene signaling, especially the phosphorylation-dependent cleavage from endoplasmic reticulum and nuclear movement of the EIN2-CEND peptide (Qiao *et al*. 2012). In melon overexpressing *CmNRAMP5*, the peak in the internal ethylene concentration in fruits occurred earlier than in wild type (unpublished result). SAUR71 is expressed in the steles of young roots and hypocotyls, and is differentially expressed during stomatal formation (Qiu *et al*. 2013). *LAX2* is an auxin-responsive and/or auxin-related gene, and is strongly expressed in the primary root cap, where it is involved in specification of the quiescent center in *Arabidopsis* (Saito *et al*. 2019). PYL proteins are ABA receptors in *Arabidopsis*, and ABA perception by PYR/PYLs plays a major role in the regulation of seed germination and establishment (Gonzalez-Guzman *et al*. 2012). PYL1 inhibits protein phosphatase-type 2C upon binding of pyrabactin, an ABA agonist, whereas PYL2 appears relatively insensitive to this compound (Yuan *et al*. 2010).

The CDC5L protein is a core component of the putative E3 ubiquitin ligase complex, which plays roles in pre-messenger RNA splicing and in the cellular response to DNA damage. Recent studies have described a new function for CDC5L in the regulation of the ATR-mediated cell-cycle checkpoint in response to genotoxic agents (Zhang *et al*. 2009). It has been reported that CDC5 is involved in the ABA-mediated flooding tolerance of soybean (Komatsu *et al*. 2013), and is responsible for cell division and expansion during the thickening of the taproot in radish (Xie *et al*. 2018).

AtVPS35, which is localized in the pre-vacuolar compartment and immunoprecipitates with VPS29, is involved in sorting proteins to protein storage vacuoles in seeds, possibly by recycling vacuolar sorting receptor from the prevacuolar compartment to the Golgi complex. It is also involved in plant growth and senescence in vegetative organs (Yamazaki *et al*. 2008). AtVPS29 plays an important

role in the trafficking of soluble proteins to the lytic vacuole from the trans-Golgi network to the prevacuolar compartment (Kang *et al*. 2012). The retromer components VPS35A and VPS29 are essential for normal prevacuolar compartment morphology and normal trafficking of plasma membrane proteins in plants (Nodzyński *et al*. 2013). A recent study showed that ZmVPS29 is involved in auxin accumulation during early kernel development in maize (Chen *et al*. 2020). An evolutionarily conserved VPS26 protein (VPS26C; At1G48550) functions in a complex with VPS35A and VPS29, which are necessary for root hair growth in *Arabidopsis* (Jha *et al*. 2018).

Other proteins identified in the protein–protein interaction network are known to have functions in transporting, binding, chelating, and chaperoning metal ions. These proteins had close homologs in *Arabidopsis* such as: (1) metal transporters (COPT5, YSL2); (2) enzymes involved in metal chelator synthesis (NAS1, and NAS2); (3) metal-binding proteins, including metallothionein (MT2); (4) metallochaperones (CCS); (Zlobin *et al*. 2015) and (5) metal tolerance proteins (MTPC2, MTPC4, MTP4, MTP11).

In previous studies on *Arabidopsis*, elevated Cu concentrations induced *CCS* and *YSL2* expression and inhibited *NAS2* expression in roots, and induced *CCS* and *NRAMP4* expression in leaves. In canola, Fe and Mn contents in leaves were significantly decreased when plants were treated with Cu at high concentrations. The *AtNRAMP3, AtNRAMP4* double mutant contained fewer functional photosystem II complexes, indicating that NRAMP transporters play important roles in photosystem II formation (Lanquar *et al*. 2010). Some proteins are known to interact with porphyrin and chlorophyll metabolism. Among them, CAO, which is located on the inner envelope and thylakoid membranes of chloroplasts in *Arabidopsis* and barley, was able to catalyze the conversion of chlorophyllide a to chlorophyllide b *in vitro* (Reinbothe *et al*. 2006). Genetic studies have shown that ChlM is critical for chlorophyll biosynthesis and chloroplast development in tobacco and *Arabidopsis* (Alawady and Grimm 2005; Pontier *et al*. 2007). Proteins with phosphatidylinositol binding activity include SNX1, whose expression is induced by salt. This protein has NO synthase-like activity and produces NO under salt stress, which plays a crucial role in the development of salt tolerance (Li *et al*. 2018)

Under Fe deficiency, exogenous NaCl was shown to promote the reutilization of cell wall Fe, and participate in the translocation of Fe from roots to shoots in *Arabidopsis*, partially because of its effects on ABA content. This was associated with the up-regulation of genes encoding proteins related to the long-distance transport of Fe, such as NAS1 (Nicotianamine Synthase1), YSL2 (Yellow Stripe-Like) and FRD3 (Ferric Reductase Defective3) (Zhu *et al*. 2017).

HMA3 encodes heavy metal ATPase 3, which is responsible for cadmium (Cd) detoxification. In *Sedum plumbizincicola*, *SpHMA3* was found to be highly expressed in shoots and its encoded protein was localized to the tonoplast (Liu *et al*. 2017). Overexpression of *OsHMA3* increased Cd tolerance, and the plants produced rice grains with almost no Cd, also had little effect on grain yield or on the concentrations of Zn, Fe, Cu, and Mn (Lu *et al*. 2019).

A previous transcriptome study suggested that oxidative stress and protein denaturation are important contributors to arsenic (As) and Cd toxicity (Verbruggen *et al*. 2009). Phosphate (P) fertilizers are widely used in modern agriculture to improve crop growth. A higher P supply increases As and Cd uptake in shoots and roots, and excess heavy metals increase oxidative damage mediated by reactive oxygen species (ROS). The ROS are generated as a by-product of physiological reactions such as electron flow in chloroplasts and mitochondria and some redox reactions. The first line of defense against ROS is SODs, a group of metalloenzymes that include Cu/Zn SOD, Mn SOD, and Fe SOD (Ozturk *et al*. 2010; Kung *et al*. 2014). Exposure to Cd was shown to increase the expression of *SOD* genes in rice, but SOD expression in shoots and roots was found to decrease when rice plants were exposed to Cd without a phosphorus (P) supply, resulting in oxidative damage (Wang *et al*. 2015). Other studies have shown that P deficiency affects Fe storage, as indicated by the accumulation of Fe associated with ferritin in chloroplasts. Inside chloroplasts, the expression of the ferritin gene, *AtFer1*, is regulated by the phosphate starvation response transcription factor AtPHR1, but this transcription factor does not affect the transcription of *ITR1*, which encodes a protein involved in Fe-uptake (Hirsch *et al*. 2006; Bournier *et al*. 2013). In soybean, most *NRAMP* genes displayed contrasting responses to Fe and sulfur deficiencies (Qin *et al*. 2017). The ATX1-like domain at the N terminus is essential for the Cu chaperone function of AtCCS *in planta*; this protein is essential for the integration of Cu into Cu/Zn SOD (Chu *et al*. 2005).

Conclusion

In this study, we identified the members of the *NRAMP* gene family in melon. Our results showed that only CmNRAMP5 has all the characteristic motifs, while the other five CmNRAMP have shorter amino acid sequences. The presence of particular *cis*-acting elements in the *CmNRAMP* promoter sequences and the expression patterns of the genes under different treatments, as verified by qPCR, indicate that the members of the *NRMAP* gene family respond to different plant hormones and metal ions. A protein–protein interaction analysis indicated that melon NRAMPs functions as metal ion transporters and interact with proteins involved in SOD activity, plant hormone signal transduction, signal transduction by protein phosphorylation, and nicotianamine synthase activity. This study provides insights into the diversity of melon NRAMPs, and provides baseline data for further comprehensive and in-depth analyses of their functions.

Acknowledgement

We acknowledge the financial support of the National Natural Science Foundation of China (No.31660577), Natural Science Foundation of Inner Mongolia Autonomous Regin (2020MS03013) and Program for Young Talents of Science and Technology in Universities of Inner Mongolia Autonomous Region (No. NJYT-19-B19). The English text of a draft of this manuscript was edited by Jennifer Smith, PhD, from Liwen Bianji, Edanz Group China.

Author Contributions

Agula Hasi and Feng Gao conceived and designed the experiments; Yufeng Zhuang and Lan Jin performed the experiments; Bayaer Enhe analyzed the data; Lan Jin wrote the paper.

References

Alawady AE, B Grimm (2005). Tobacco Mg protoporphyrin IX methyltransferase is involved in inverse activation of Mg porphyrin and protoheme synthesis. *Plant J* 41:282–290

Alejandro S, R Cailliatte, C Alcon, L Dirick, F Domergue, D Correia, L Castaings, JF Briat, S Mari, C Curie (2017). Intracellular distribution of manganese by the trans-Golgi network transporter *NRAMP2* is critical for photosynthesis and cellular redox homeostasis. *Plant Cell* 29:3068–3084

Bailey TL, M Bodén, FA Buske, M Frith, CE Grant, L Clementi, J Ren, WW Li, WS Noble (2009). MEME SUITE: tools for motif discovery and searching. *Nucl Acids Res* 37:202–208

Bie Z, MA Nawaz, Y Huang, JM Lee, G Colla (2017). Introduction to vegetable grafting. *In: Vegetable Grafting. Principles and Practices*, pp: 1–21. Colla G, FP Alfocea, D Schwarz (Eds.). CABI Publishing, Wallingford, UK

Bournier M, N Tissot, S Mari, J Boucherez, E Lacombe, JF Briat, F Gaymard (2013). Arabidopsis ferritin 1 (*AtFer1*) gene regulation by the phosphate starvation response 1 (AtPHR1) transcription factor reveals a direct molecular link between iron and phosphate homeostasis. *J Biol Chem* 288:22670–22681

Cailliatte R, A Schikora, JF Briat, S Mari, C Curie (2010). High-affinity manganese uptake by the metal transporter *NRAMP1* is essential for Arabidopsis growth in low manganese conditions. *Plant Cell* 22:904–917

Cailliatte R, B Lapeyre, JF Briat, S Mari, C Curie (2009). The *NRAMP6* metal transporter contributes to cadmium toxicity. *Biochem J* 422:217–228

Chen C, H Chen, Y He, R Xia (2018). TBtools, a toolkit for biologists integrating various HTS-data handling tools with a user-friendly interface. *bioRxiv* 2018; Article 289660

Chen L, YX Li, C Li, Y Shi, Y Song, D Zhang, H Wang, Y Li, T Wang (2020). The retromer protein *ZmVPS29* regulates maize kernel morphology likely through an auxin-dependent process(es). *Plant Biotechnol J* 18:1004–1014

Chu CC, WC Lee, WY Guo, SM Pan, LJ Chen, H Li, TL Jinn (2005). A copper chaperone for superoxide dismutase that confers three types of copper/zinc superoxide dismutase activity in *Arabidopsis*. *Plant Physiol* 139:425–436

Colangelo EP, ML Guerinot (2006). Put the metal to the petal: Metal uptake and transport throughout plants. *Curr Opin Plant Biol* 9:322–330

Ezura H, WO Owino (2008). Melon, an alternative model plant for elucidating fruit ripening. *Plant Sci* 175:121–129

Fleming MD, CC Trenor, MA Su, D Foernzler, DR Beier, WF Dietrich, NC Andrews (1997). Microcytic anaemia mice have a mutation in Nramp2, a candidate iron transporter gene. *Nat Genet* 16:383–386

Gao F, Y Niu, J Hao, R Bade, L Zhang, A Hasi (2013). Identification of genes differentially expressed during ethylene climacteric of melon fruit by suppression subtractive hybridization. *J Integr Agric* 12:1431–1440

Gao H, W Xie, C Yang, J Xu, J Li, H Wang, X Chen, CF Huang (2018). *NRAMP2*, a trans-Golgi network-localized manganese transporter, is required for Arabidopsis root growth under manganese deficiency. *New Phytol* 217:179–193

Gonzalez-Guzman M, GA Pizzio, R Antoni, F Vera-Sirera, E Merilo, GW Bassel, MA Fernández, MJ Holdsworth, MA Perez-Amador, H Kollist, PL Rodriguez (2012). Arabidopsis PYR/PYL/RCAR receptors play a major role in quantitative regulation of stomatal aperture and transcriptional response to abscisic acid. *Plant Cell* 24:2483–2496

Hirayama T, JM Alonso (2000). Ethylene captures a metal! metal ions are involved in ethylene perception and signal transduction. *Plant Cell Physiol* 41:548–555

Hirsch J, E Marin, M Floriani, S Chiarenza, P Richaud, L Nussaume, MC Thibaud (2006). Phosphate deficiency promotes modification of iron distribution in *Arabidopsis* plants. *Biochimie* 88:1767–1771

Huang Y, W Li, L Zhao, T Shen, J Sun, H Chen, Q Kong, MA Nawaz, Z Bie (2016). Melon fruit sugar and amino acid contents are affected by fruit setting method under protected cultivation. *Sci Hortic* 214:288–294

Ishida JK, DGG Caldas, LR Oliveira, GC Frederici, LMP Leite, TS Mui (2018). Genome-wide characterization of the NRAMP gene family in Phaseolus vulgaris provides insights into functional implications during common bean development. *Genet Mol Biol* 41:820–833

Jha SG, ER Larson, J Humble, DS Domozych, DS Barrington, ML Tierney (2018). Vacuolar protein sorting 26C encodes an evolutionarily conserved large retromer subunit in eukaryotes that is important for root hair growth in *Arabidopsis thaliana*. *Plant J* 94:595–611

Kang H, SY Kim, K Song, EJ Sohn, Y Lee, DW Lee, I Hara-Nishimura, I Hwang (2012). Trafficking of vacuolar proteins: the crucial role of *Arabidopsis* vacuolar protein sorting 29 in recycling vacuolar sorting receptor. *Plant Cell* 24:5058–5073

Komatsu S, C Han, Y Nanjo, M Altaf-Un-Nahar, K Wang, D He, P Yang (2013). Label-free quantitative proteomic analysis of abscisic acid effect in early-stage soybean under flooding. *J Proteom Res* 12:4769–4784

Kung CP, YR Wu, H Chuang (2014). Expression of a dye-decolorizing peroxidase results in hypersensitive response to cadmium stress through reducing the ROS signal in *Arabidopsis*. *Environ Exp Bot* 101:47–55

Lanquar V, MS Ramos, F Lelièvre, H Barbier-Brygoo, A Krieger-Liszkay, U Krämer, S Thomine (2010). Export of vacuolar manganese by *AtNRAMP3* and *AtNRAMP4* is required for optimal photosynthesis and growth under manganese deficiency. *Plant Physiol* 152:1986–1999

Lanquar V, F Lelièvre, S Bolte, C Hamès, C Alcon, D Neumann, G Vansuyt, C Curie, A Schröder, U Krämer, H Barbier-Brygoo, S Thomine (2005). Mobilization of vacuolar iron by *AtNRAMP3* and *AtNRAMP4* is essential for seed germination on low iron. *EMBO J* 24:4041–4051

Lescot M, P Déhais, G Thijs, K Marchal, Y Moreau, VVD Peer, P Rouzé, S Rombauts (2002). PlantCARE, a database of plant cis-acting regulatory elements and a portal to tools for in silico analysis of promoter sequences. *Nucl Acids Res* 30:325–327

Letunic I, P Bork (2018). 20 years of the SMART protein domain annotation resource. *Nucl Acids Res* 46:493–496

Li JY, J Liu, D Dong, X Jia, SR McCouch, LV Kochian (2014). Natural variation underlies alterations in Nramp aluminum transporter (*NRAT1*) expression and function that play a key role in rice aluminum tolerance. *Proc Natl Acad Sci USA* 111:6503–6508

Li TT, WC Liu, FF Wang, QB Ma, YT Lu, TT Yuan (2018). SORTING NEXIN 1 functions in plant salt stress tolerance through changes of NO accumulation by regulating NO synthase-like activity. *Front Plant Sci* 9; Article 1634

Liu H, H Zhao, L Wu, A Liu, F J Zhao, W Xu (2017). Heavy metal ATPase 3 (HMA3) confers cadmium hypertoleranceon the cadmium/zinc hyperaccumulator *Sedum plumbizincicola*. *New Phytol* 215:687–698

LuC, L Zhang, Z Tang, X Huang, J Ma, F Zhao (2019). Producing cadmium-free Indica rice by overexpressing *OsHMA3*. *Environ Intl* 126:619–626

Mani A, K Sankaranarayanan (2018). *In silico* analysis of natural resistance-associated macrophage protein (NRAMP) family of transporters in rice. *Protein J* 37:237–247

Meng JG, XD Zhang, SK Tan, KX Zhao, ZM Yang (2017). Genome-wide identification of Cd-responsive *NRAMP* transporter genes and analyzing expression of *NRAMP* 1 mediated by miR167 in *Brassica napus*. *Biometals* 30:917–931

Nevo Y, N Nelson (2006). The NRAMP family of metal-ion transporters. *Biochim Biophys Acta* 1763:609–620

Nodzyński T, MI Feraru, S Hirsch, RD Rycke, C Niculaes, W Boerjan, JV Leene, GD Jaeger, S Vanneste, J Friml (2013). Retromer subunits VPS35A and VPS29 mediate prevacuolar compartment (PVC) function in *Arabidopsis*. *Mol Plant* 6:1849–1862

Ozturk F, F Duman, Z Leblebici, R Temizgul (2010). Arsenic accumulation and biological responses of watercress (*Nasturtium officinale* R. Br.) exposed to arsenite. *J Exp Bot* 69:167–174

Pan H, Y Wang, Q Zha, M Yuan, L Yin, T Wu, X Zhang, X Xu, Z Han (2015). Iron deficiency stress can induce *MxNRAMP1* protein endocytosis in *M. xiaojinensis*. *Gene* 567:225–234

Pech JC, M Bouzayen, A Latchq (2008). Climacteric fruit ripening: ethylene-dependent and independent regulation of ripening pathways in melon fruit. *Plant Sci* 175:114–120

Peris-Peris C, A Serra-Cardona, F Sánchez-Sanuy, S Campo, J Ariño, BS Segundo (2017). Two *NRAMP6* isoforms function as iron and manganese transporters and contribute to disease resistance in rice. molecular plant-microbe interactions. *Mol Plant Microb* 30:385–398

Pontier D, C Albrieux, J Joyard, T Lagrange, MA Block (2007). Knock-out of the magnesium protoporphyrin IX methyltransferase gene in *Arabidopsis*: effect on chloroplast development and on chloroplast-to-nucleus signaling. *J Biol Chem* 282:2297–2304

Qiao H, Z Shen, S Carol Huang, RJ Schmitz, MA Urich, SP Briggs, JR Ecker (2012). Processing and subcellular trafficking of ER-tethered EIN2 control response to ethylene gas. *Science* 338:390–393

Qin L, P Han, L Chen, TC Walk, Y Li, X Hu, L Xie, H Liao, X Liao (2017). Genome-wide identification and expression analysis of *NRAMP* family genes in soybean (*Glycine max* L.). *Front Plant Sci* 8; Article 1436

Qiu T, Y Chen, M Li, Y Kong, Y Zhu, N Han, H Bian, M Zhu, J Wang (2013). The tissue-specific and developmentally regulated expression patterns of the *SAUR41* subfamily of small auxin up RNA genes: potential implications. *Plant Signal Behav* 8; Article e25283

Reinbothe C, S Bartsch, LL Eggink, JK Hoober, J Brusslan, R Andrade-Paz, J Monnet, S Reinbothe (2006). A role for chlorophyllide a oxygenase in the regulated import and stabilization of light-harvesting chlorophyll a/b proteins. *Proc Natl Acad Sci USA* 103:4777–4782

Saito T, P Opio, S Wang, K Ohkawa, S Kondo, T Maejima, H Ohara (2019). Association of auxin, cytokinin, abscisic acid, and plant peptide response genes during adventitious root formation in Marubakaido apple rootstock (*Malus prunifolia* Borkh. var. ringo Asami). *Acta Physiol Plantarum* 41; Article 41

Sasaki A, N Yamaji, K Yokosho, JF Ma (2012). Nramp5 is a major transporter responsible for manganese and cadmium uptake in rice. *Plant Cell* 24:2155–2167

Shannon P, A Markiel, O Ozier, NS Baliga, JT Wang, D Ramage, N Amin, B Schwikowski, T Ideker (2003). Cytoscape: A software environment for integrated models of biomolecular interaction networks. *Genomic Res* 13:2498–2504

Supek F, L Supekova, H Nelson, N Nelson (1996). A yeast manganese transporter related to the macrophage protein involved in conferring resistance to mycobacteria. *Proc Natl Acad Sci USA* 93:5105–5110

Szklarczyk D, AL Gable, D Lyon, A Junge, S Wyder, J Huerta-Cepas, M Simonovic, NT Doncheva, JH Morris, P Bork, LJ Jensen, C von Mering (2019). STRING v11: protein-protein association networks with increased coverage, supporting functional discovery in genome-wide experimental datasets. *Nucl Acids Res* 47:607–613

Tamura K, D Peterson, N Peterson, G Stecher, M Nei, S Kumar (2011). MEGA5: Molecular evolutionary genetics analysis using maximum likelihood, evolutionary distance, and maximum parsimony methods. *Mol Biol Evol* 28:2731–2739

Tang QY, CX Zhang (2013). Data Processing System (DPS) software with experimental design, statistical analysis and data mining developed for use in entomological research. *Ins Sci* 20:254–260

Verbruggen N, C Hermans, H Schat (2009). Mechanisms to cope with arsenic or cadmium excess in plants. *Curr Opin Plant Biol* 12:364–372

Vidal SM, D Malo, K Vogan, E Skamene, P Gros (1993). Natural resistance to infection with intracellular parasites: isolation of a candidate for Bcg. *Cell* 73:469–485

Wang H, T Wang, I Ahmad (2015). Involvement of phosphate supplies in different transcriptional regulation pathway of *Oryza sativa* L.'s antioxidative system in response to arsenite and cadmium stress. *Ecotoxicology* 24:1259–1268

Xia J, N Yamaji, T Kasai, JF Ma (2010). Plasma membrane localized transporter for aluminum in rice. *Proc Natl Acad Sci USA* 107:18381–18385

Xiao H, L Yin, X Xu, T Li, Z Han (2008). The iron-regulated transporter, *MbNRAMP1*, isolated from Malus baccata is involved in Fe, Mn and Cd trafficking. *Ann Bot* 102:881–889

Xie Y, L Xu, Y Wang, L Fan, Y Chen, M Tang, X Luo, L Liu (2018). Comparative proteomic analysis provides insight into a complex regulatory network of taproot formation in radish (*Raphanus sativus* L.). *Hortic Res* 5:51–64

Xiong H, T Kobayashi, Y Kakei, T Senoura, M Nakazono, H Takahashi, H Nakanishi, H Shen, P Duan, X Guo, N Nishizawa, Y Zuo (2012). *AhNRAMP1* iron transporter in involved in iron acquisition in peanut. *J Exp Bot* 63:4437–4446

Xiong M, X Zhang, S Shabala, L Shabala, Y Chen, C Xiang, MA Nawaz, Z Bie, H Wu, H Yi, M Wu, Y Huang (2018). Evaluation of salt tolerance and contributing ionic mechanism in nine Hami melon landraces in Xinjiang, China. *Sci Horitc* 237:277–286

Yamaji N, A Sasaki, JX Xia, K Yokosho, JF Ma (2013). A node-based switch for preferential distribution of manganese in rice. *Nat Commun* 4; 2442

Yamazaki N, T Shimada, H Takahashi, K Tamura, M Kondo, M Nishimura, I Hara-Nishimura (2008). *Arabidopsis* VPS35, a retromer component, is required for vacuolar protein sorting and involved in plant growth and leaf senescence. *Plant Cell Physiol* 49:142–156

Yuan X, P Yin, Q Hao, C Yan, J Wang, N Yan (2010). Single amino acid alteration between valine and isoleucine determines the distinct pyrabactin selectivity by PYL1 and PYL2. *J Biol Chem* 285:28953–28958

Zha Q, Y Wang, XZ Zhang, ZH Han (2014). Both immanently high active iron contents and increased root ferrous uptake in response to low iron stress contribute to the iron deficiency tolerance in *Malus xiaojinensis*. *Plant Sci* 214:47–56

Zhang N, R Kaur, S Akhter, RJ Legerski (2009). Cdc5L interacts with ATR and is required for the S-phase cell-cycle checkpoint. *EMBO Rep* 10:1029–1035

Zheng Y, S Wu, Y Bai, H Sun, C Jiao, S Guo, ZK Hao, J Blanca, Z Zhang, S Huang, Y Xu, Y Weng, M Mazourek, UK Reddy, K Ando, JD McCreight, AA Schaffer, J Burger, Y Tadmor, N Katzir, X Tang, Y Liu, JJ Giovannoni, KS Ling, WP Wechter, A Levi, J Garcia-Mas, R Grumet, Z Fei (2019). Cucurbit Genomics Database (CuGenDB): a central portal for comparative and functional genomics of cucurbit crops. *Nucl Acids Res* 47:1128–1136

Zhu XF, Q Wu, L Zheng, RF Shen (2017). NaCl alleviates iron deficiency through facilitating root cell wall iron reutilization and its translocation to the shoot in *Arabidopsis thaliana*. *Plant Soil* 417:155–167

Zlobin IE, VP Kholodova, ZF Rakhmankulova, VV Kuznetsov (2015). *Brassica napus* responses to short-term excessive copper treatment with decrease of photosynthetic pigments, differential expression of heavy metal homeostasis genes including activation of gene *NRAMP4* involved in photosystem II stabilization. *Photosynth Res* 125:141–150